NURETH14-33

LARGE EDDY AND INTERFACE SIMULATION (LEIS) OF LIQUID ENTRAINMENT IN TURBULENT STRATIFIED FLOW

S. Gulati¹, J. Buongiorno¹ and D.Lakehal^{1,2}

¹ Massachusetts Institute of Technology, Cambridge, Massachusetts, USA
² ASCOMP GmbH, Zurich, Switzerland

Abstract

Dryout of the liquid film on the fuel rods in BWR fuel assemblies leads to an abrupt decrease in heat transfer coefficient and can result in fuel failure. The process of mechanical mass transfer from the continuous liquid field into the continuous vapor field along the liquid-vapor interface is called entrainment and is the dominant depletion mechanism for the liquid film in annular flow. Using interface tracking methods combined with a Large Eddy Simulation approach, implemented in the Computational Multi-Fluid Dynamics (CMFD) code TransAT®, we are studying entrainment phenomena in BWR fuel assemblies. In this paper we report on the CMFD simulation approaches and the current validation effort for the code.

1. Introduction

Dryout is defined as the condition in annular flow when there is complete evaporation of liquid film on the wall surface. This leads to an abrupt decrease in the heat transfer coefficient and hence is not a desired condition in Boiling Water Reactors (BWR). Dryout may take place in two-phase flows with high flow quality. A number of semi-empirical correlations for prediction of dryout have been proposed in the literature [1] and will be reviewed in Section 2 below. Most of these correlations make use of simplified assumptions, such as idealized interface geometries. The correlations are used as constitutive relations for the interfacial exchange terms in the phase-averaged, two- or three-field model [2]. It is noted that an accurate prediction of the dryout condition in BWRs could lead to higher safety margins and/or core power rates. Clearly, there is a strong incentive for conducting further research to develop more accurate models for dryout.

The liquid layer depletion leading to dryout in annular flow is due to two processes: a) Entrainment and, b) Evaporation. On the other hand, the liquid film is replenished by droplet deposition from the vapor phase to the liquid phase. Entrainment refers to the process of mechanical mass transfer from the continuous liquid field into the dispersed droplet field along an interface. Entrainment is typically the dominant depletion mechanism for the liquid film under BWR operational conditions. Therefore, we have chosen this phenomenon as the starting point for the development of a more general, high-fidelity modeling framework of dryout.

It is clear that the liquid/vapor interface geometry plays a major role in modeling the dryout phenomenon. Interface Tracking Methods (ITM) can capture the interface geometry accurately and also be used to predict the velocity and temperature gradients at the interfacial scale, which is necessary to estimate the rate of inter-phase heat/mass transfer. Although this approach can be computationally expensive, it eliminates the need of using empirical models for interfacial mass,

momentum and scalar exchange terms. A number of studies have been carried out with the ITM approach [3]., which we have applied in this work to predict entrainment phenomenon.

One of the most commonly used ITMs is the level set method [4]. The level set method essentially solves only one set of Navier-Stokes equations for a fluid with density, viscosity and other properties discontinuous and piecewise functions of space. The interface topology is tracked by solving an advection equation for a continuous marker function, whose zero-value contour defines the interface location. The method is in principle capable of predicting the formation of interfacial features rather accurately. Rodriguez [5] used a level set approach implemented in the PHASTA–IC code to predict entrainment in annular flow and was able to capture the physics of the problem such as ligament formation and droplet shearing. It is also noted that flow conditions inside a BWR fuel assembly are highly turbulent, which makes a Direct Numerical Simulation (DNS) of turbulence approach computationally very expensive. Therefore, the LEIS (Large Eddy Interface Simulation) approach, as described by [6], is adopted. LEIS amounts to a combination of an accurate ITM formulation within an explicit Large-Eddy Simulation (LES) algorithm; LEIS is useful for high Reynolds number interfacial flows.

In this work, the code TransAT® developed by ASCOMP GmbH is used for carrying out the simulations [6]. The code's general features are described in Section 3.1. In Sections 3.2, the interface tracking and turbulence modeling capabilities of the code are tested, respectively, with a benchmark case of two-dimensional wavy falling liquid films [7], and a benchmark case of single-phase turbulent channel flows [8]. Finally, in Section 4 some preliminary results for stratified flow at BWR pressure and flow conditions are shown.

2. Entrainment in Annular Flows

2.1 The Mechanism:

Annular flows are typical of channels with very high vapor superficial velocities, yielding liquid entrainment, driven by the formation of small roll waves on top of large disturbance waves on the liquid film [9]. The roll waves are essentially a result of Kelvin-Helmholtz instabilities on the surface of disturbance waves due to velocity shear. This leads to formation of ligaments. The ligaments eventually disintegrate into droplets when the interfacial shear velocity becomes very large and dominates other forces acting on the interface such as surface tension and gravity. It is noted here that the liquid droplets entrained by the gaseous phase may re-enter the liquid film via deposition, which acts as a counter phenomenon to entrainment. At fully-developed flow conditions (possible only in an adiabatic channel), the amount of entrainment is equal to the amount of deposition.

2.2 Empirical Models:

It is common to model annular flows using multi-field models [10, 11]. The multi-field models basically involve solving the mass, energy and momentum conservation equations for each phase separately. The interaction between the phases is taken into account by adding heat, mass and momentum transfer exchange terms. These exchange terms are modelled using empirical correlations: For example, Kataoka and Ishii [12] and Ishii and Mishima [13] proposed correlations for entrainment rates in equilibrium (fully-developed) zones and under-entrained

zone, as well as the entrainment fraction and entrance length required to reach the equilibrium conditions. Ishii and Mishima [13] also provided correlations for predicting the droplet size distribution and critical velocity for onset of entrainment.

Lopez de Bertodano et al. [14] proposed a correlation for entrainment rate which is said to provide a better agreement than the Kataoka and Ishii correlation for high pressure and large gas mass flow rates. Pan and Hanratty [15] proposed a correlations for the prediction of equilibrium entrainment fraction and the critical gas superficial velocity required for onset of entrainment

Dallman et al. [16] Kataoka et al. [17] and Okawa et al. [18] proposed correlations for the atomization and deposition coefficients of droplets. In addition, Secondi [1] recommend using Okawa et al. [18] correlation for assessment of droplet entrainment for BWR rod bundles. In traditional multi-field models (such as those used in codes like RELAP5), these correlations are used to provide closure relations for the conservation equations.

The problem with this approach is that the correlations are either completely empirical or based on oversimplifying assumptions about the interface topology and mass, momentum and energy exchange at the interface. To achieve high fidelity prediction of dryout, more accurate closure relations are needed. In the remainder of this paper, we discuss how interface tracking methods can be used for modeling annular flows and ultimately obtaining high-fidelity closure relations for multi-field codes.

3. TransAT – Code Description and Benchmark Cases

3.1 TransAT® multiphase flow software:

The CMFD code TransAT® developed by ASCOMP, Switzerland, is a multi-physics, finite volume code based on solving multifluid Navier-Stokes equations. The code uses structured meshes, though allowing for multiple blocks to be set together. MPI (Message Passing Interface) parallel based algorithm is used in connection with multi-blocking. The grid arrangement is collocated and can thus handle more easily curvilinear skewed grids. The solver is pressure based, corrected using a density-correction technique to account for compressibility. High-order time marching and convection schemes can be employed; up to third order monotone schemes in space. Multiphase flows are tackled using interface tracking techniques for both laminar and turbulent flows. Specifically, both the level set and volume of fluid methods can be employed to track evolving interfaces.

3.2 Benchmark Cases:

3.2.1 Two Dimensional Wavy Liquid Film Falling Under Gravity:

In order to benchmark TransAT for multiphase modelling and interface tracking capabilities, a benchmark case of two dimensional wavy liquid film falling under gravity is used. It is noted that the velocity shear at the interface between the liquid phase and the gaseous phase deforms the surface. The physics concerning this phenomenon is very similar to droplet entrainment as it involves large interfacial deformations, thus making it an ideal benchmark case for investigation of multiphase modelling and interface tracking capabilities.

A detailed study for the falling liquid film has been carried by Nave [19]. A similar study is performed with TransAT. The computational data are compared with experiments of Nosoko et al. [7]. In order to effectively compare the codes, similar dimensionless groups for describing the properties, interface wavelengths and Reynolds numbers are used [7]:

$$N_f = \frac{\rho^3 \nu^4 g}{\sigma^3} \tag{1}$$

$$N_{hp} = h_{peak} \left(\frac{v^2}{g}\right)^{-\frac{1}{3}} \tag{2}$$

$$N_{\lambda} = \lambda_{s} \left(\frac{v^{2}}{g}\right)^{-\frac{1}{3}} \tag{3}$$

Here N_f , N_{hp} and N_{λ} are the non-dimensional fluid property group, non-dimensional peak height (amplitude) and non-dimensional wavelength, respectively, ρ is the density of liquid, ν is the kinematic viscosity of liquid, g is the acceleration due to gravity, h_{peak} is the peak height and λ_s is the wavelength of the waves at steady state observed in experiments. The velocity scale is defined by

$$V = (\nu g)^{1/3} \tag{4}$$

The Reynolds number is calculated based on undisturbed film thickness h_0 and is given by:

$$Re = \frac{Vh_0}{V} \tag{5}$$

Nosoko et al. [7] also propose the following empirical correlation for predicting the amplitude of the observed wavelengths for laminar two dimensional falling wavy liquid films:

$$N_{hp} = 0.49 N_f^{0.044} N_{\lambda}^{0.39} Re^{0.46} \tag{6}$$

Figures 1a, 1b and 1c show typical wave profiles obtained by TransAT and schematic of profile observed by Nosoko et al. [7]. Roll waves and capillary waves can be clearly seen in each of these cases. The simulations for TransAT were run for a 56x256 grid with 56 points in the wall normal direction and 256 points in the streamwise direction. The level set equation is advected using the 3rd order Quick scheme, combined with the 3rd order WENO scheme for its reinitialization [20]. The maximum and minimum CFL limits used were 1.3 and 0.8. The boundary conditions are set to periodic in the streamwise direction and no-slip in the wall normal direction. The convergence is achieved when the wave amplitudes achieve steady state.

Table 1 shows the computation matrix and the results obtained from the simulations. The Reynolds number based on initial film thickness, liquid property group and the dimensionless wavelength is specified and the dimensionless peak heights are computed from the simulation and compared with the experimental correlation (equation 6). All physical properties, except surface tension, are the same as that of water for liquid and air for gaseous phase at atmospheric

pressure. This fixes the velocity scale (as defined by equation 4) and hence the initial (undisturbed) film thickness is calculated based on the Reynolds number to be used. The surface tension is varied to obtain different N_f .

The Reynolds number corresponds to laminar flow regime. The dimensionless peak height group from the experimental correlation of Nosoko et al. [7] and the code TransAT is computed and compared. It can be observed from Table 1 that TransAT gives relatively small deviations from the correlations of Nosoko et al. [7].

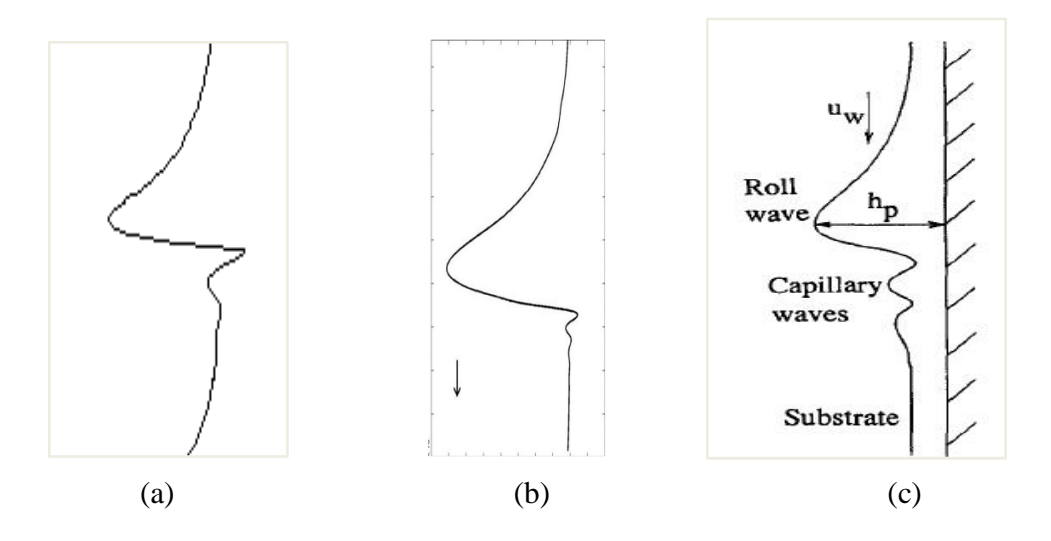


Figure 1: Typical wave profile obtained with (a) TransAT, (b) Nave [19] for case 4 in Table 1; (c) Qualitative nature of wave profile described by Nosoko et al. [7]

Table 1: Dimensionless Peak Heights calculated with TransAT

Serial	Re	$N_f \times 10^{-12}$	N_{λ}	N_{hp} from	N_{hp} (TransAT with	N_{hp} (TransAT with
No.				Nosoko et al.	implicit surface	explicit surface
					tension	tension
					formulation)	formulation)
1	20	43.88	626.2	8.388	7.821	7.227
2	40	0.1614	689.4	9.360	9.247	Wave Breaks
3	50	0.2018	742.6	10.783	9.371	n/a
4	103	0.0520	994.9	15.876	13.284	n/a
5	103	0.4100	994.9	17.386	17.013	16.683

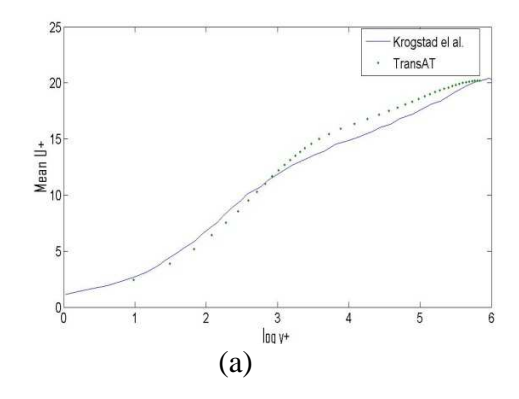
Another feature of the code is the implementation of an implicit surface tension formulation, which allows use of fewer time steps, thus speeding up the simulation. The implicit formulation also improves accuracy as seen by a comparison with the explicit formulation for the same grid sizes (see Table 1, two rightmost columns). The explicit surface tension formulation in space and time for capillary flows imposes a restriction on minimum grid size and time step. However, the implicit surface tension formulation is stronger as it does not lead to such a restriction. In the

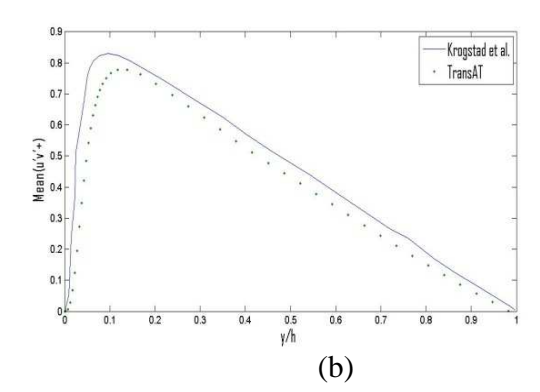
given numerical limits, it was found that the implicit surface tension formulation was more accurate than the explicit one.

3.2.2 Large Eddy Simulation of Single Phase Channel Flow:

In order to assess TransAT's predictive capabilities as to turbulence, a benchmark case of single phase flow in a horizontal channel is used. Numerical simulations for this case have been carried out by a number of researchers [8, 21]. For the purpose of comparison, the LES simulation is performed for a bulk Reynolds number of 6300 (corresponding to a shear Reynolds number $Re_{\tau} = 400$) and compared with the DNS of Krogstad et al. [8]. The computational domain used is $4\pi h * 2\pi h * 2h$ and the grid size is 111 x 92 x 92 (streamwise x spanwise x wall normal direction). Here, h is the channel half width. The boundary conditions are periodic in the streamwise and spanwise directions and no slip in the wall normal direction. The grid was created using the grid generator TransATMesh included in TransAT. The grid is staggered, Cartesian with uniform cell dimensions in streamwise and spanwise direction, and refined near the wall with a maximum and minimum ratio of 3 and 1.1 between the cell dimensions (in the wall normal direction). For the purpose of computation, an explicit Range-Kutta 3rd order time scheme is used. The maximum and minimum CFL limits are 0.1 and 0.3. The turbulent kinetic energy of the liquid in channel was used as an indicator of convergence. The convergence is achieved when the turbulent kinetic energy achieves a statistically steady state.

The results for normalized velocities and normalized Reynolds stress components are shown in Figure 2. The sub-grid scale model used in these LES is based on the eddy viscosity kernel by reference to Smagorinsky, combined with near-wall damping of turbulence using a harmonic mean between the Prandtl mixing-length defined by (κ y), where κ is the von Karman constant and y is the wall distance, and (Cs Δ), where Cs is the SGS model constant and Δ is the filter width. The quantities plotted in the figure below are scaled using the frictional velocity $u_{\tau} = \sqrt{\tau_w/\rho}$, and plotted versus either the viscous length scale $y^+ = \frac{u_{\tau}y}{v}$, or y/h, where h is the half channel width It is seen that a reasonable agreement between LES and DNS is achieved; noting the selected shear Reynolds number is actually pretty high for the computational grid.





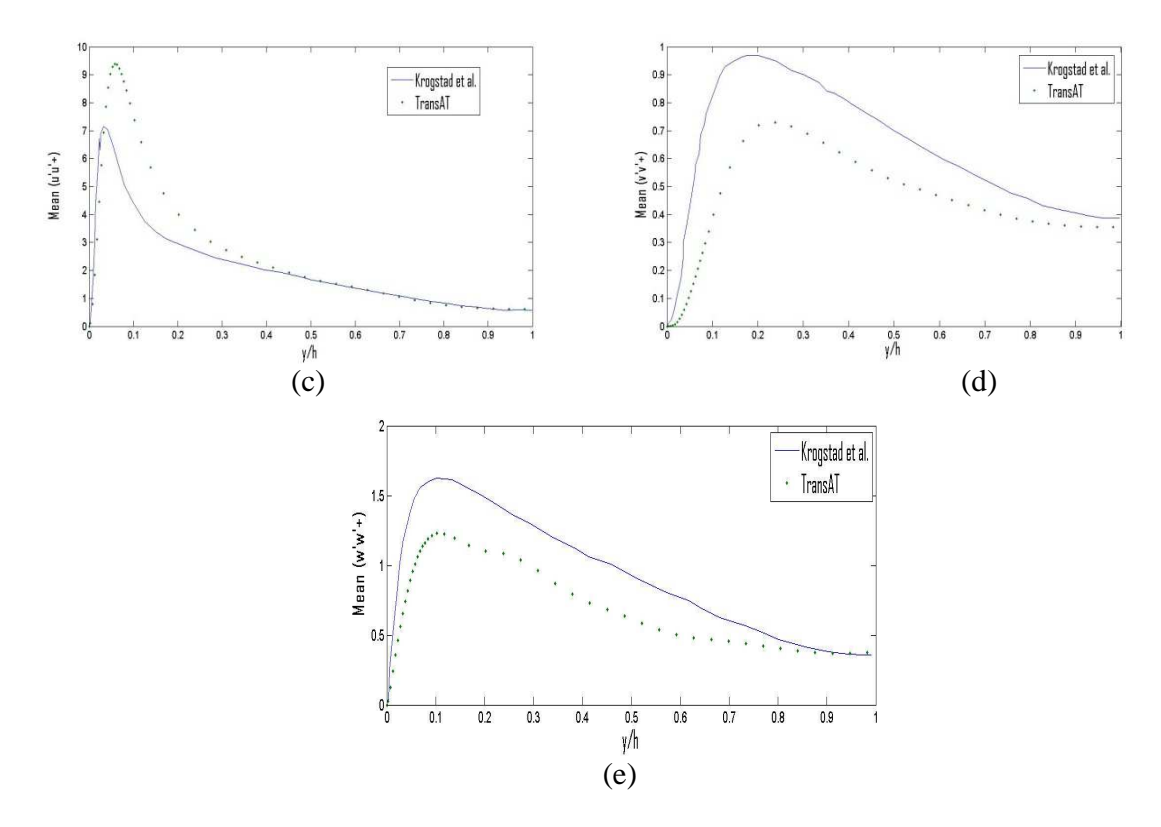


Figure 2: Normalized velocity profiles and Reynolds stress components obtained with LES in TransAT compared with DNS by Krogstad et al. [8]

4. Entrainment Modelling in TransAT

For the following simulations, the geometry used is a horizontal channel. An explicit numerical scheme with LEIS is used. An adaptive time stepping scheme is used with maximum and minimum CFL limits being 0.1 and 0.3. The boundary conditions are set to periodic in streamwise direction to keep the domain size computationally tractable and periodic in spanwise direction to allow for accurate turbulent modelling near the wall. The boundary condition in the wall normal direction is set to no-slip. The use of periodic conditions in the streamwise direction entails a zero pressure gradient in the streamwise direction, which is clearly unphysical. In order to force the flow, an artificial source term is added such that it tends to keep the volume averaged liquid and vapor superficial velocity constant (equal to a pre-specified value). In other words, the liquid and vapor superficial velocities are specified as input to the simulation. The domain is initialized with a slightly perturbed film corresponding to the expected void fraction. The convergence is achieved when the artificial source term and the turbulent kinetic energy become statistically steady. In the following subsections, the characteristics of CFD simulation parameters for different flow regimes are identified and discussed.

4.1 Horizontal Stratified Flow Simulations:

As a starting point, stratified flow is modelled for air-water mixture. The results are validated using measurements of Shi and Kocamustafaogullari [22]. It is noted that Shi and

Kocamustafaogullari measured the interfacial parameters in stratified flows in horizontal pipes. However, the simulations are carried out for channel flow geometry (with the same hydraulic diameter) due to their ease of meshing and implementation in TransAT. It is noted that the difference in geometry does not affect the physics of the flow.

Shi and Kocamustafaogullari conducted experiments for a 0.0503 mm inner diameter pipe having a length of 15.4 m and characterized the flow into six regimes based on superficial velocities. Figure 3 represents the flow regime map as described by Shi and Kocamustafaogullari [21] – 2D represents 2-Dimensional, LA represents Large Amplitude and AT represents Atomization. The gas superficial velocity is denoted by Jg and liquid superficial velocity is described by Jf. To validate the simulations, the wavelength and wave speed measured from the simulations are compared with the results of Shi and Kocamustafaogullari [21]. Figure 4 shows the wavelength and wave speed as observed by Shi and Kocamustafaogullari for different superficial velocities. In the following subsections, we present the results obtained for 2D regime and Large Amplitude regime identifying the challenges introduced in determining the size of computational domain for each regime. The challenges introduced in modelling the atomization regime are discussed in section 4.2.

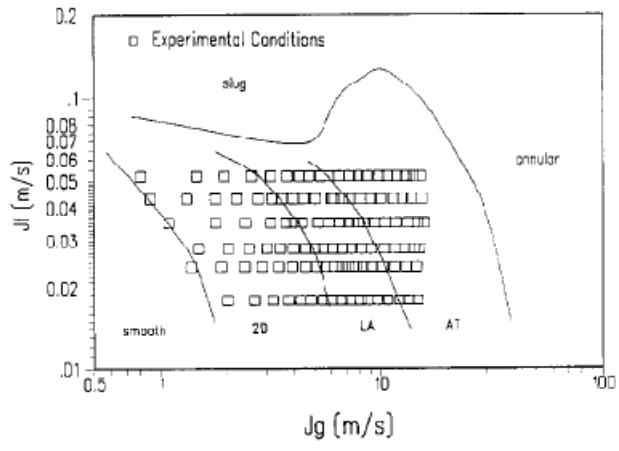
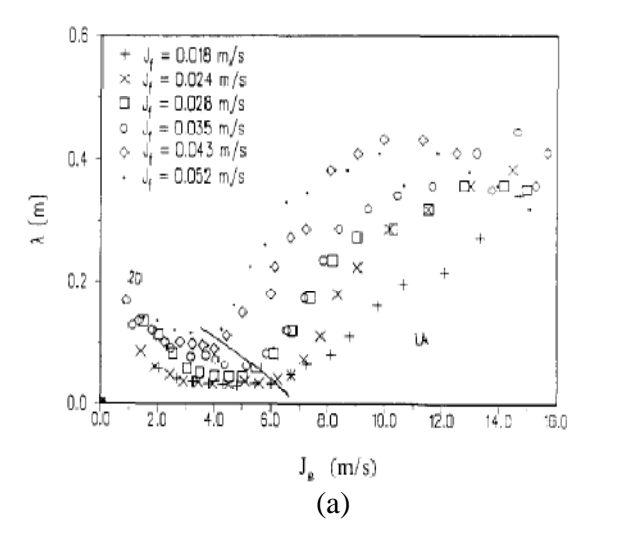


Figure 3: Flow regime map (taken from Shi and Kocamustafaogullari [21])



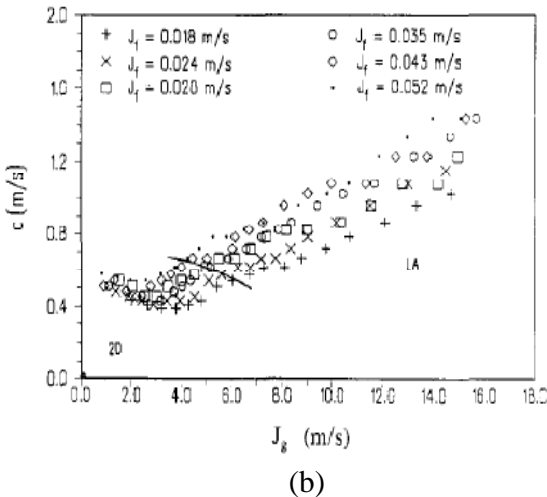


Figure 4: a) Mean Wavelength, b) Mean Wave Velocity for different gas superficial velocities (taken from Shi and Kocamustafaogullari [21])

4.1.1 2-D Regime:

The vapor superficial velocity is kept at 2 m/s while the liquid superficial velocity is kept as 0.028 m/s. It can be seen from figure 3 that this falls in the 2D regime. From figure 4a, it can be seen that the expected wavelength is 0.11 m. This leads to a choice of domain of length 0.12 m in the streamwise direction. The grid used is 100 x 100 x 25 (streamwise x wall normal x spanwise). It is noted that the number of grid points limits the computational resources and hence longer domains (implying larger number of grid points) cannot be used. The choice of domain length is strictly governed by the expected wavelength. A coarse grid is used in the spanwise directions because 2D nature of the flow is expected from experiments. A square cross section of the channel with the side of square equal to 0.0503 m is used noting that the hydraulic diameter for such a configuration is also 0.0503 m which is same as the diameter of the pipe used in Shi and Kocamustafaogullari [21].

The wavevelocity computed from the simulation in the converged state is 0.6 m/s while it is expected to be 0.5 m/s from Figure 4b and hence shows relatively good agreement. Furthermore, as shown in figure 5a, the domain consists of only 1 wave spanning its entire length and hence corresponding to a wavelength of 0.12m which is in relatively good agreement with Figure 4a.

4.1.2 Large Amplitude Regime:

The vapor superficial velocity is kept at 6.8 m/s while the liquid superficial velocity is kept at 0.024 m/s. As can be seen from Figure 3, this corresponds to Large Amplitude regime. The expected mean wavelength as seen from Figure 4a is 0.04 m. This leads to a choice of domain of length 0.1 m in the streamwise direction with a grid of 100 x 100 x 100. It is noted that in this case a three dimensional film is expected and hence the grid in spanwise direction is finer than section 4.1.1. The cross section is same as the one described for 2D regime. The wave velocity computed from the simulation is 0.8 m/s and expected from the experiment is 0.6 m/s. At the final converged state (shown in figure 5b), the mean wavelength observed from the experiment is 0.035m and the expected wavelength from the experiment is 0.04 m. It can be seen that a relatively good agreement is observed between the experiments and simulated data.

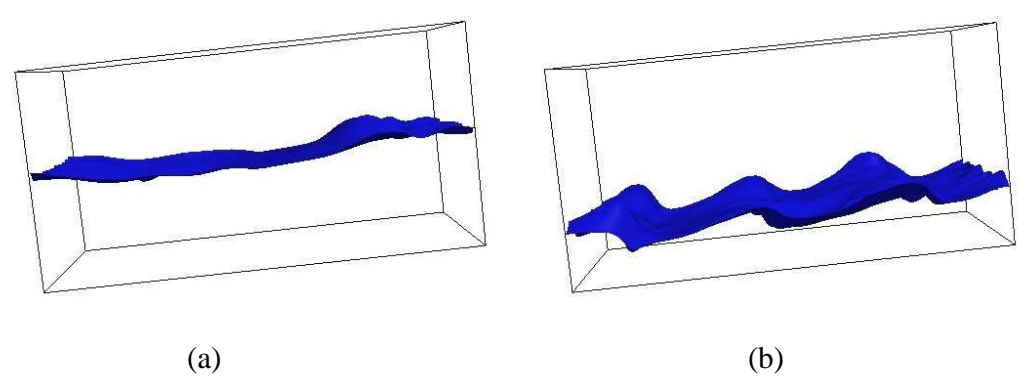


Figure 5: Wave profile for a) 2-D regime, b) Large Amplitude Regime

4.2 Horizontal Annular Flow Simulations:

From the above section, it is clear that the wavelength plays an important role in determining the length of the computational domain in the streamwise direction. From Figure 3 and Figure 4a, it can be inferred from the trends that the wavelengths are significantly large for the atomization and annular flow regime. Hence, these regimes require a long domain and hence a larger number of grid points and large computation resources.

As a starting point for modelling annular flows, liquid entrainment for steam-water mixture at 7 MPa in a horizontal channel is modelled. The domain length is 0.01 m in the wall normal direction, 0.02 m in the spanwise direction and 0.025 m in the streamwise direction. The grid is 100 x 100 x 125 (wall normal x spanwise x streamwise). The length of the domain is less than the wavelength of disturbance waves observed from the experiments. The average superficial velocities of both phases are fixed (1.5 and 20 m/s for the liquid and vapor phase, respectively). Figure 6 and Figure 7 show a snapshot of the 3D interface geometry and cross-sectional profiles for a preliminary simulation. The gravity is along negative Y direction, X is the streamwise direction and Z is the spanwise direction. In the figure, ligament formation and droplet entrainment are clearly visible. It can be seen that we start with a horizontal stratified flow which rapidly develops with time into annular flow and a film is formed on the top surface, which is physically correct. This simulation was carried out on an 8 core 3.00 GHz Intel Xeon CPU X5472 machine with 16 GB RAM. It is planned to implement this simulation on a 64 node cluster as it would enable simulating a complete wavelength in about 1 month.

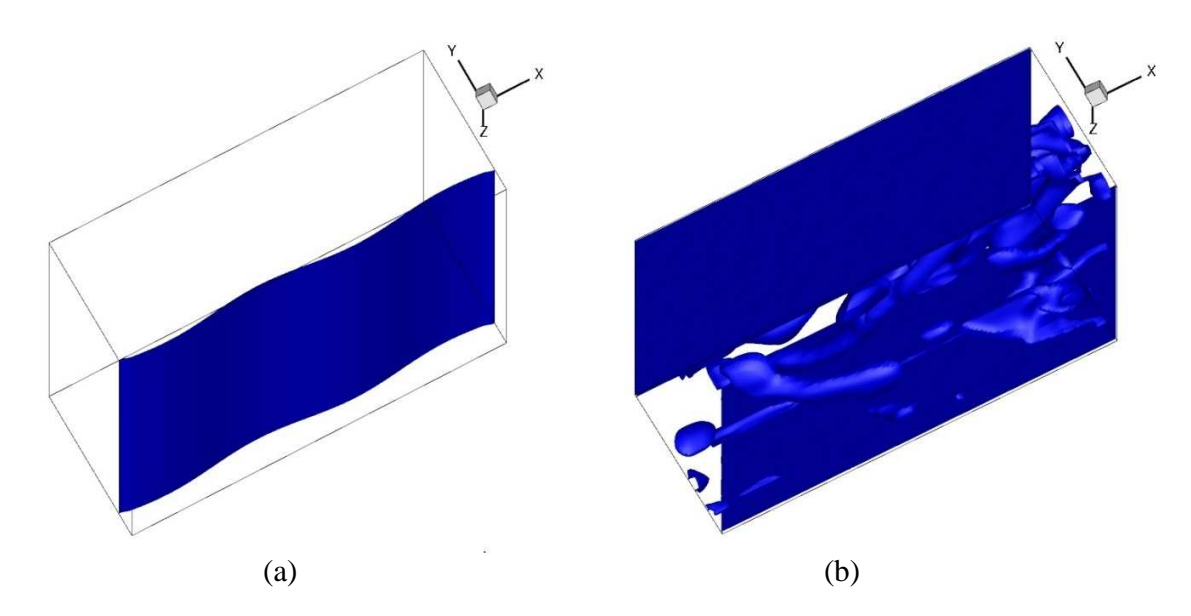


Figure 6: Snapshot of interface geometry for preliminary simulation at a) t=0 ms, b) t=120 ms. The iso-surface corresponds to the interface between liquid and gas phase.

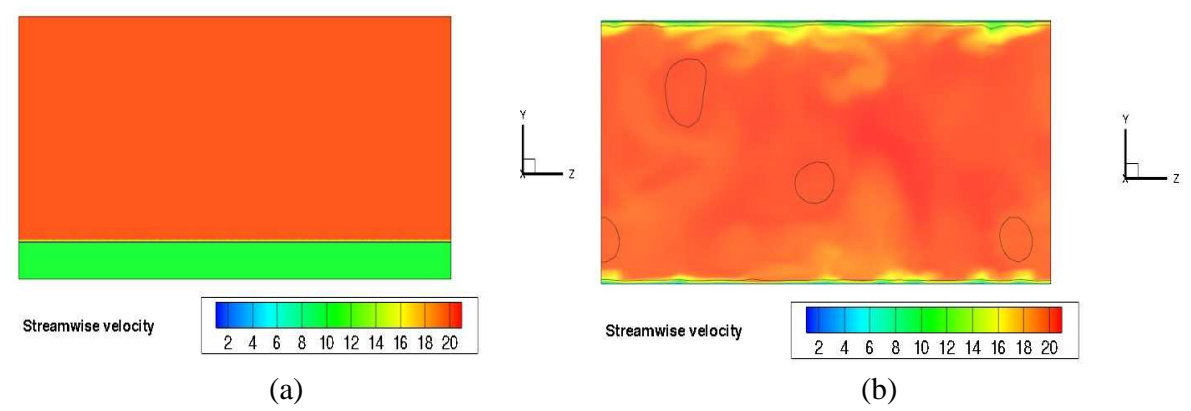


Figure 7: Cross-sectional velocity profiles for preliminary simulation at a) t=0 ms, b) t=120 ms. The phase distribution is also shown: it suggests the presence of a liquid film on the top and bottom walls, as well as large liquid droplet entrained by the vapour core.

5. Conclusion

A Computational Multiphase Fluid Dynamics based simulation framework of liquid entrainment in BWRs is being developed using a combination of LES for turbulence and ITM for interface evolution. The simulations are performed with the code TransAT. In this study, the interface tracking and turbulence modeling capabilities of TransAT were tested using representative benchmark cases of two dimensional wavy falling liquid films with large interfacial deformation, single phase channel flows and horizontal stratified flows. In all cases, the code predictions agreed well with data from literature. Current work is focusing on the use of a combined interface tracking and LES to simulate droplet entrainment in more prototypical BWR conditions. In order to validate the models, an experimental facility with particle image velocimetry (PIV) capabilities is being constructed and will be tested soon.

6. Acknowledgements

This work is supported by the Tokyo Electric Power Company (TEPCO). The authors would like to express their gratitude towards Dr. Despoina Chatzikyriakou and Dr. Chidambaram Narayanan for their constant support and guidance.

7. References

- [1] Secondi, F., (2009), An Assessment of Entrainment Correlations for the Dryout Prediction in BWR Fuel Bundles, 13th International Topical Meeting on Nuclear Reactor Thermal Hydraulics (NURETH-13).
- [2] Hoyer, N., (1998), Calculation of dryout and post-dryout heat transfer for tube geometry, *International Journal of Multiphase Flow, Volume 24, Issue 2, Pages 319-334.*
- [3] Prosperetti, A. and Tryggvason, G., (2007), Computational Methods for Multiphase Flow, *Cambridge University Press*.
- [4] Lakehal, D., Meier, M., Fulgosi, M., (2002), Interface tracking towards the direct simulation of heat and mass transfer in multiphase flows, *International Journal of Heat and Fluid Flow*, 23, pp. 242-257.

- [5] Rodriguez, J.M., (2009), Numerical Solution of Two Phase Annular Flow, *PhD Thesis*, *Rensselaer Polytechnic Institute*.
- [6] Lakehal, D., (2008), LEIS for the Prediction of Turbulent Multifluid Flows with and without Phase Change Applied to Thermal Hydraulic Applications, *XCHD4NRS OCDE Conf.*, *Grenoble*.
- [7] Nosoko, T., Yoshimura, P.N., Nagata, T., Oyakawa, K., (1996), Characteristics of Two Dimensional Waves on a Falling Liquid Film, *Chemical Engineering Science*, Vol. 51, Issue 5, pp. 725-732.
- [8] Krogstad, P.A., Andersson, H.I., Bakken, O.M., Ashrafian, A., (2005), An experimental and numerical study of channel flow with rough walls, *Journal of Fluid Mechanics, Vol. 530*, pp. 327-352.
- [9] Woodmansee, D.E. and Hanratty, T.J., (1969), Mechanism for the removal of droplets from a liquid surface by a parallel air flow, *Chemical Engineering Science*, Vol. 24 (2), pp. 299-307.
- [10] Patruno, L.E., Marchetti, J.M., Jakobsen, H.A., Svendsen, H.F., (2009), Modeling of Droplet Entrainment in Annular Two Fluid Three Phase Dispersed Flow, 13th International Topical Meting on Nuclear Reactor Thermal Hydraulics (NURETH-13).
- [11] Corre, J.M.L. and Adamsson, C., (2009), Development of a New Mechanistic Tool for the Prediction of Liquid Film Dryout During a Transient, 13th International Topical Meting on Nuclear Reactor Thermal Hydraulics (NURETH-13).
- [12] Kataoka, I. and Ishii, M., (1983), Entrainment and Deposition Rates for Droplets in Annular Two Phase Flow, *ASME-JSME Thermal Engineering Joint Conference, Honolulu, Hawaii*
- [13] Ishii, M. and Mishima, K., (1984), Two Fluid Model and Hydrodynamic Constitutive Relation, *Nuclear Engineering and Design*, 82 (2-3), pp. 107-126.
- [14] Lopez de Bertodano, M.A., Assad, A., Beus, S., (1998), Entrainment rate of droplets in the ripple annular regime for small vertical ducts, *Nuclear Science and Engineering*, *Vol. 129* (1), pp. 72-80.
- [15] Pan, L., Hanratty, Thomas J., (2002), Correlation of entrainment for annular flow in vertical pipes, *International Journal of Multiphase Flow*, 28, 363-384.
- [16] Dallman, J.C., Jones, B.G., Hanratty, Thomas J., (1979), Interpretation of entrainment measurements in annular gas-liquid flows, *AIChE Symp. Ser 2*, 68-76.
- [17] Kataoka, I., Ishii, M., Nakayama, A., (2000), Entrainment and deposition rates of droplets in annular two phase flow, *International Journal of Heat and Mass Transfer*, 43, 1573-1589.
- [18] Okawa, T., Kotani, A., Kataoka, I., Naitoh, M., (2004), Prediction of the critical heat flux in annular regime in various vertical channels, *Nuclear Engineering Design*, 229, pp. 223-236.
- [19] Nave, J.C., (2004), Direct Numerical Simulation of Liquid Films, *PhD Thesis, University of California Berkeley*.
- [20] Jiang, Guang-Shan and Shi, Chi-Wang, (1996), Efficient Implementation of Weighted ENO Schemes, *Journal of Computational Physics*, 126, pp. 202-228.
- [21] Kravchenko, A.G., Moin, P., Moser, R., (1996), Zonal Embedded Grids for Numerical Simulations of Wall-Bounded Turbulent Flows, *Journal of Computational Physics*, 127, pp. 412-423.
- [22] Shi, J. and Kocamustafaogullari, G., (1994), Interfacial Measurements in Stratified Flow Patterns, *Nuclear Engineering and Design 149*, pp. 81.